

Central European Journal of Chemistry

Preparation and characterization of new hydrogels based on poly(vinyl alcohol)/phosphoester chondroitin sulphate

Research Article

Tachita Vlad-Bubulac*, Diana Serbezeanu#, Ana-Maria Oprea, Ionela-Daniela Carja, Corneliu Hamciuc, Maria Cazacu

> "Petru Poni" Institute of Macromolecular Chemistry. lasi-700487, Romania

Received 15 June 2012; Accepted 19 November 2012

Abstract: New polymer hydrogels based on partially phosphorylated poly(vinyl alcohol) (PVA/Phosphoester) have been prepared. Fourier transform infrared spectroscopy (FT-IR) was employed to confirm PVA/Phosphoester formation. Contact angle measurements were performed to evaluate the surface characteristics of the hydrogels. The PVA/Phosphoester hydrogels were co-networked with Chondroitin sulfate (CS) in various ratios by chemical crosslinking. The synthetic-natural mixed resulted semi-IPN hydrogels were structurally and morphologically investigated by ATR - FT-IR spectroscopy and scanning electron microscopy, respectively. The swelling behavior and dynamic moisture sorption capacity of the PVA/Phosphoester (p-methyl-phenyl phosphonic dichloride) (P3)-CS semi-IPN hydrogels were followed. It was found that the performance of the semi-IPN hydrogels was influenced by the CS. By kinetic studies, it has been shown that the swelling processes occurred by an anomalous transport mechanism.

Keywords: Polymer gels • Poly(vinyl alcohol) • Phosphorylated poly(vinyl alcohol) • Chondroitin sulphate • Swelling behavior © Versita Sp. z o.o.

1. Introduction

The term hydrogel is used to describe materials that are three-dimensional, hydrophilic, polymeric networks capable of retaining a large amount of water [1,2]. The hydrogels' characteristics, including sensitivity to the environment, tissue-like water content and elasticity afford their potential use in biomedical applications. Hydrogels have important applications in the areas of controlled drug delivery, such as coatings in pharmaceutical applications and as dissolution and binding agents in tablets [3,4]. The main disadvantage of hydrogels is their poor mechanical properties after swelling. To overcome this drawback, hydrogels can be modified by physical blending with polymeric matrices having better mechanical stability [5-7] or/and chemical modification by grafting [8-10], interpenetrating polymer networks (IPN) [11] and the crosslinking method [12]. The formation of IPNs represents an important method

to improve the mechanical strength of polymers due to physical entanglements and network interactions when compared to individual polymers [13].

Poly(vinyl alcohol) (PVA) is a polymer of great interest due to its many desirable characteristics which allow its use in various pharmaceutical and biomedical applications [14]. PVA has the ability to form hydrogels due to its ability to easily form intra/intermolecular interactions via hydrogen bonding. There are well known methods to prepare hydrogels based on PVA. The freezethawing method is often used to enhance the mechanical properties of hydrogels [15]. PVA hydrogels are also prepared by chemical crosslinking using irradiation or crosslinkers, such as glutaraldehyde or boric acid and sodium borate, but, for pharmaceutical applications, especially when PVA is used as a carrier in drug delivery, the residual crosslinking agents, eventually present in the final hydrogel, could alter the biological activity or degrade the biologically active agent being released.

To overcome such inconveniences other less toxic crosslinking agents should be developed [16,17]. The use of PVA as the main component for hydrogels formation is particularly advantageous, due to the abundance of hydroxyl pendant groups on the PVA chains that can be further substituted with various functional groups. Several research groups have investigated the addition of methacrylate and acrylate pendant groups [18-20], chitosan [21], sulfosalicylic acid [22], hydroxyapatite [23], and alginate [24]. The versatility of PVA hydrogels makes them materials of choice for many biomedical applications, as matrices for cell immobilization and for the controlled release of drugs [25,26].

Polyphosphoesters (PPEs) represent a wide class of biodegradable polymers with repeating phosphoester linkages in the backbone, where the phosphorus atom is pentavalent and it thereby allows the introduction of bioactive molecules and extensive modification of the physical and chemical properties of these polymers [27,28]. PPEs are known to be biodegradable [29] and biocompatible [27] and they are widely used in drug [30,31], protein [27] or gene delivery [32,33] and tissue engineering [34].

In the past partially phosphorylated poly(vinyl alcohol) has attracted considerable interest because of its nonflammability [35,36], its ability to form metal complexes [37], anionic polyelectrolyte hydrogels [38-40] and to obtain cationic exchanged resins [41]. Recently, phosphorylated poly(vinyl alcohol) has been taken into consideration for biological applications [42]

Chondroitin sulfate (CS) is a polysaccharide present in the extracellular matrix of cartilages and tissues of the body, serving both important structural and biological functions. CS provides compressive strength to connective tissues by regulating their water content, and possesses characteristic features suitable for bioapplications [2,43-45]. However, the readily water-soluble nature of chondroitin sulphate limits its applicability as solid-state drug delivery vehicle. Therefore, some crosslinking treatments were taken into consideration to tailor the properties of chondroitin sulphate in order to produce more stable materials.

Actually, blending monomeric and polymeric precursors is a well-established route in the design of functional materials. Herein, our aim was to combine the multifunctionality and biodegradability characteristics of chondroitin sulphate with the adjustable mechanical strength of PVA tailored by chemical crosslinking with adequate ratios of phosphoester functions. Thus, the present study describes the preparation of PVA/PPEs—CS semi-IPNs by the chemical crosslinking of PVA *via* phosphonic dichloride polycondensation, followed by

the epichlorohydrin-crosslinking of PVA/PPEs and CS. The semi-IPN hydrogels were characterized by FT-IR spectroscopy. The effect of CS content in the semi-IPN hydrogel on water absorption and water vapor transport rates was determined.

2. Experimental procedure

2.1. Materials

Poly(vinyl alcohol) (PVA) (Mw=18300 Da) was received from SC ROMCRIL Rasnov; phenyl dichlorophosphate, phenylphosphonic dichloride and epichlorohydrin were purchased from Sigma-Aldrich; chondroitin sulfate (CS) powder, (Mw = 35 kDa) was obtained from Roth (Germany). p-Methyl-phenyl phosphonic dichloride was synthesized from p-methyl-dichlorophosphine and purified by distillation under reduced pressure according to the method reported in the literature [46]. Cyclohexyl phosphonic dichloride was prepared starting from PCI, and cyclohexane by bubbling a stream of oxygen, under vigorous stirring, as described in the literature [47]. Phosphate buffer solution (PBS) was prepared from phosphate buffered saline by dissolution in distilled water. All other reagents were used as received from commercial sources or were purified by standard methods.

2.2. Measurements 2.2.1. FT-IR spectroscopy

Fourier transform infrared (FT-IR) spectra were registered on a Bruker Vertex 70 (Bruker, Germany) either in transmission mode, at frequencies ranging from 400 to 4000 cm⁻¹ (with a resolution of 2 cm⁻¹ and accumulation of 32 scans), or in reflexion mode, in the 600-4000 cm⁻¹ spectral range (64 scans, at 2 cm⁻¹ resolution). A Golden Gate ATR accessory (Specac Ltd.) was used in the latter case. The single reflection IRE was diamond, with an incidence angle of 45°.

2.2.2. Contact angle measurements

The contact angle measurements were performed by using CAM-PLUS Micro apparatus. Measurements were made using liquid distilled water (density 0.9986 g cm⁻³) and ethanol (density 0.7894 g cm⁻³) in air (density 0.0013 g cm⁻³) at room temperature (T = 20°C). Drops with small volume were used to minimize the effects of gravitation. Scans made every 5 seconds in the range 0-45 seconds were collected.

2.2.3. Scanning electron microscopy

Scanning electron microscopy (SEM) was performed on a TESLABS 301 instrument, at 25 kV, with a magnification

Scheme 1. The synthetic route of PVA/PPE (P1-P4).

of 380-3600. The images were taken on film surfaces deposed on Al supports and coated by sputtering with Au thin films using an EK 3135 EMITECH device.

2.2.4. Swelling tests

Swelling studies were performed for all formulations and carried out by direct immersion in PBS, pH 7.4. The hydrogel samples were maintained for 24 hours at 37 °C; they were periodically removed from the solution, gently wiped with a soft tissue to remove surface solution, weighed and then placed back into the vessel as quickly as possible. The swelling degree at equilibrium was calculated according to the Eq. 1:

$$Q_{max}(\%) = (W_t - W_d)/W_d \ 100 \tag{1}$$

where W_t is the weight of the swollen samples at time t and W_d is the weight of the dry sample.

To determine the kinetics of solvent diffusion into the matrices (swelling), the following Eq. 2 was used [48]:

$$F_t = \frac{W_t}{W_{eq}} = k_{sw} t^{n_{sw}} \tag{2}$$

where W_t and W_{eq} represent the amount of 7.4 PBS solution, absorbed by the matrices at time t and at equilibrium, respectively; k_{sw} is the swelling constant characteristic for the system and n_{sw} is the power law diffusion exponent, which takes into account the type of solvent transport. Eq. 2 is applied to initial states of

swelling (swelling degree less than 60%) and linearity is observed when $\log F_t$ as a function of $\log t$ is represented.

2.2.5. Dynamic water vapors sorption

Water vapor absorption capacity of the film samples was measured by using the fully automated gravimetric analyzer IGAsorp supplied by Hiden Analytical, Warrington (UK). An ultrasensitive microbalance measures the weight change as the humidity is modified in the sample chamber at a constant regulated temperature. The measurement system is controlled by a user-friendly software package.

2.3. Procedure

2.3.1. Preparation of PVA/Phosphoester networks

The PVA/PPE (P1-P4) networks have been prepared by a nucleophilic displacement reaction of phosphonic dichloride with the hydroxyl groups of PVA according to a method reported in [49] using dimethylformamide as a reaction medium. The synthetic route of PVA/PPE (P1-P4) is illustrated in Scheme 1. The experimental details are described below using PVA/PPE (P3) as an example. 0.209 g (1 mmol) of *p*-methyl-phenyl phosphonic dichloride and 109.8 g (6 mmol) PVA were dissolved in 50 mL of dry dimethylformamide and the reaction mixture was kept at 90°C for 12 h with constant stirring. After that the solvent was removed under reduced pressure, and the resulted product was dried

at 50°C in a vacuum oven. The final PVA/PPE networks were purified by dialysis against water during 5 days followed by lyophilization. The yields of PVA/PPE were P1=77%, P2=80%, P3=89% and P4=85%.

2.3.2. Preparation of PVA/Phosphoester (P3)—CS hydrogels

The PVA/PPE (P3) based on *p*-methyl-phenyl phosphonic dichloride was chosen further in order to synthesize PVA/PPE (P3)–CS mixed hydrogels.

Thus, PVA/PPE (P3) and CS were dispersed in various weight ratios (90/10, 80/20, 70/30, 60/40, 50/50) in aqueous alkaline solution (NaOH 9%), in presence of epichlorohydrin under vigorous stirring. The obtained gel-like samples were placed on glass plates and the crosslinking reaction was completed by heating at 80°C for 8 h. Hydrogels were extensively washed with water to remove the unreacted compounds. The samples were dried for 10 h by using a LABCONCO FreeZone device.

3. Results and discussion

3.1. FT-IR spectroscopy for PVA/Phosphoester (P1-P4) networks

The structure of the resulting compounds was investigated by FT-IR spectroscopy. Fig. 1 shows the FT-IR spectrum of PVA/PPE (P3) in comparison with the FT-IR spectrum of pristine PVA. In the PVA spectrum, characteristic peaks at 3390 cm⁻¹ (O–H stretching vibration), 2931 cm⁻¹ (C–H stretching), 1733 cm⁻¹ (residual acetate CH₃COO⁻) and 1430 cm⁻¹ (C–H bending) can be observed [50]. In the spectrum of PVA/PPE (P3) the absorption bands associated with P=O (1262 cm⁻¹), P–Ar (1470 cm⁻¹), CH, CH₂ and CH₃ (2960, 2922 cm⁻¹) can be identified [51,52]. The absorption bands at 969 cm⁻¹ and 1180, 1150 cm⁻¹ prove the formation of the P–O–alkyl bonds [51,52]. Due to its bifunctionality, it is expected that PPE acts as a crosslinker between PVA polymer chains.

3.2. Contact angle measurements for PVA/ Phosphoester (P1-P4) networks

A biomaterial is any synthetic or natural material which in contact with living tissues and biological fluids does not produce an immunological or inflammatory response. Neumann demonstrated the role of surface free energy and of blood-biomaterial interfacial tension in the adhering process of sanguine plateles [53]. The methods used to determine the surface tension are based on contact angle measurements between the liquid meniscus and PVA/PPE (P1–P4) films surfaces. The surface of the material is the first component of the implant that comes

into contact with the biological cells or biological fluids. Thus, biocompatibility will be influenced primarily by the surface characteristics of the biomaterial, particularly by the wettability, surface chemistry of the exposed atoms, surface energy and surface topography. A characteristic that significantly influences this response is that related to surface wettability, which is often determined by measuring the contact angle of the material [54,55]. For the calculation of the surface tension parameters, the geometric mean method was used:

$$\frac{1+\cos\theta}{2} \frac{\gamma_{b}}{\sqrt{\gamma_{d}^{p}}} = \sqrt{\gamma_{sv}^{p}} \sqrt{\frac{\gamma_{b}^{p}}{\gamma_{b}^{d}}} + \sqrt{\gamma_{sv}^{d}}$$
(3)

$$\gamma_{sv} = \gamma_{sv}^d + \gamma_{sv}^p \tag{4}$$

where θ is the contact angle determined for water and ethylene glycol, subscripts "Iv" and "sv" denote the interfacial liquid-vapour and surface-vapour tensions, respectively, while superscripts "p" and "d" denote the polar and disperse components, respectively, of total surface tension, $\gamma_{sv}.$

Solid-liquid interfacial tension is defined with the following equation:

$$\gamma_{SL} = \left[\left(\gamma_{b}^{p} \right)^{1/2} - \left(\gamma_{sv}^{p} \right)^{1/2} \right]^{2} + \left[\left(\gamma_{bv}^{d} \right)^{1/2} - \left(\gamma_{sv}^{d} \right)^{1/2} \right]^{2} \quad (5)$$

Free energy of hydration and interfacial tension are very important in that they determine the interaction forces between two different media and influences the following processes: stability of the colloidal aqueous suspensions, dynamics of the molecular self-assembling, wettability, spatial distribution and adhesiveness of the surfaces. The biological and chemical processes, which take place at the surface of an implant, depend on the interfacial interactions between a solid and a liquid. The surface of a biomaterial must have the ability to minimize the blood – biomaterial interfacial tension in such a way that it has a reduced capacity to adsorb proteins. Although an interfacial tension equal to zero would be ideal for realization of the blood compatibility, however this is not desirable in view of the mechanical stability of the blood - biomaterial interface. It is generally considered that the blood-biomaterial interfacial tension should be 1-3 mN m⁻¹ for a good blood – biomaterial compatibility, as well as a good mechanical stability of the interface [56]. The best value for solid-liquid interfacial tension (5.6 mN m⁻¹) was obtained for PVA/PPE (P3) composition as a result of the presence of the hydrophobic -CH₂ groups of p-methyl-phenyl phosphonic dichloride. For the other samples (P1, P2 and P4, respectively) the contact angle investigation could not be performed due to sample deterioration during the experiment.

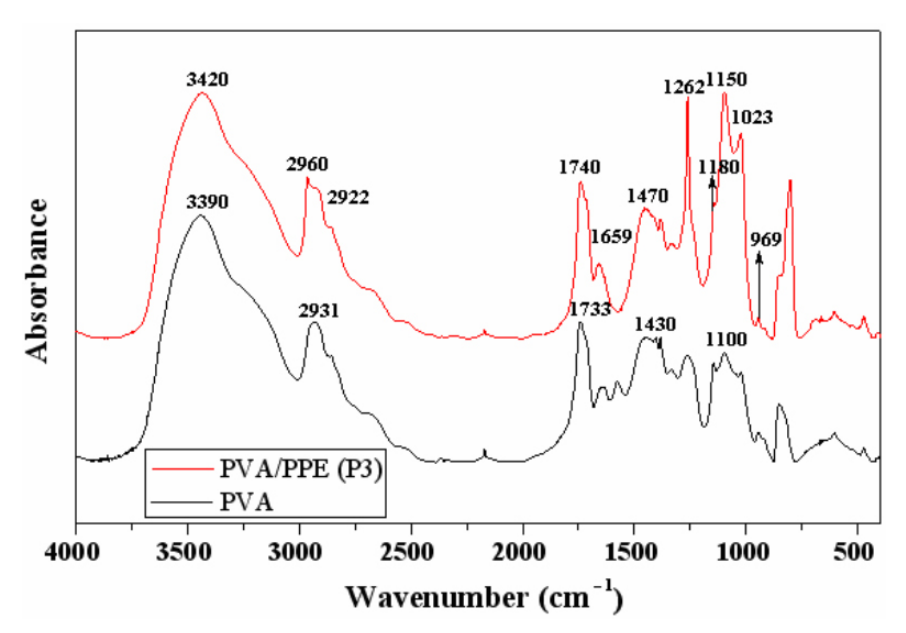


Figure 1. Comparative FT-IR spectra for PVA and PVA/PPE (P3).

3.3. Synthesis and characterization of semi-IPN hydrogels

The semi-IPN hydrogels based on PVA/PPE (P3) and CS, obtained by various mixing ratios of the components (90/10, 80/20, 70/30, 60/40, 50/50) (w/w), were properly coded as 90/10, 80/20, 70/30, 60/40, 50/50. A schematic representation of the hybrid network based on PVA/PPE (P3)—CS is shown in Fig. 2. The bonds between PVA/PPE network and CS are generated by using epichlorohydrin. The PVA/PPE (P3)—CS semi-IPN hydrogels with various mixing ratios were extensively washed with warm water in order to remove the unreacted compounds, especially epichlorohydrin traces, according to literature [57]. The yields for this semi-IPN hydrogels, presented in Table 1, ranged from 71 to ca. 78%.

3.3.1. ATR – FT-IR spectroscopy

ATR – FT-IR spectroscopy was used to assess the chemical groups characteristic for CS and PVA/PPE (P3), and to verify the formation of epichlorohydrine crosslinks. Fig. 3 shows the ATR – FT-IR spectra for the PVA/PPE (P3)–CS samples. The PVA/PPE (P3) exhibits three main absorption bands: typical strong hydroxyl bands for free alcohol (nonbonded OH stretching band) and hydrogen bonded band in the range of 3500–3100 cm⁻¹ [58], C–H stretching vibration at 2970–2850 cm⁻¹ and C–O stretching at 1100–950 cm⁻¹. Intramolecular and intermolecular hydrogen bonds are expected to occur among PVA chains due to high hydrophilic forces.

The presence of CS was evidenced by the bands at 3410–3470 cm⁻¹ which are originated from hydroxyl

groups while those at 1644 cm⁻¹–1660 cm⁻¹ by carbonyl bond of amide group. The band at 1240 cm⁻¹ corresponds to the R-OSO₂-OR [58]. Carbon-oxygen single bonds display stretching bands in the region 1200-1100 cm⁻¹. The absorption band of C-O stretching was observed at 1100 cm⁻¹. As can be observed from Fig. 3, the insertion of CS into PVA/PPE (P3) matrix did not induce significant changes in the FT-IR spectra of PVA/PPE (P3)-CS (90/10-50/50) semi-IPNs. An enlargement of the band assigned to -OH stretching according to the increase of the amount of CS in the matrix formulation was observed. Moreover, the intensity of the band at around 1650 cm⁻¹ due to the stretching vibration of carbonyl bond (amide I band) increased with increasing of CS content. The semi-IPN hydrogel was formed by the crosslinking of PVA/PPE (P3) network, while CS remained in linear form within the matrix. For this reason, significant changes between the FT-IR spectra's of PVA/ PPE (P3)-CS and PVA/PPE (P3) were not observed.

3.3.2. Scanning electron microscopy

The microstucture of the hydrogels was investigated with a scanning electron microscopy (SEM). High water contents of the hydrogels will likely result in highly macroporous sponge like scaffolds upon lyophilization. As shown in Fig. 4, all of the hydrogel samples exhibited porous structures, while pore structures are dependend on the CS content of the hydrogels. As it can be seen in Fig. 4, the pore size increased by CS incorporation. Therefore, the solvent molecules could easily diffuse into hydrogels, leading to a higher swelling ratio [45]. The high hydrophilicity of CS also contributes to this

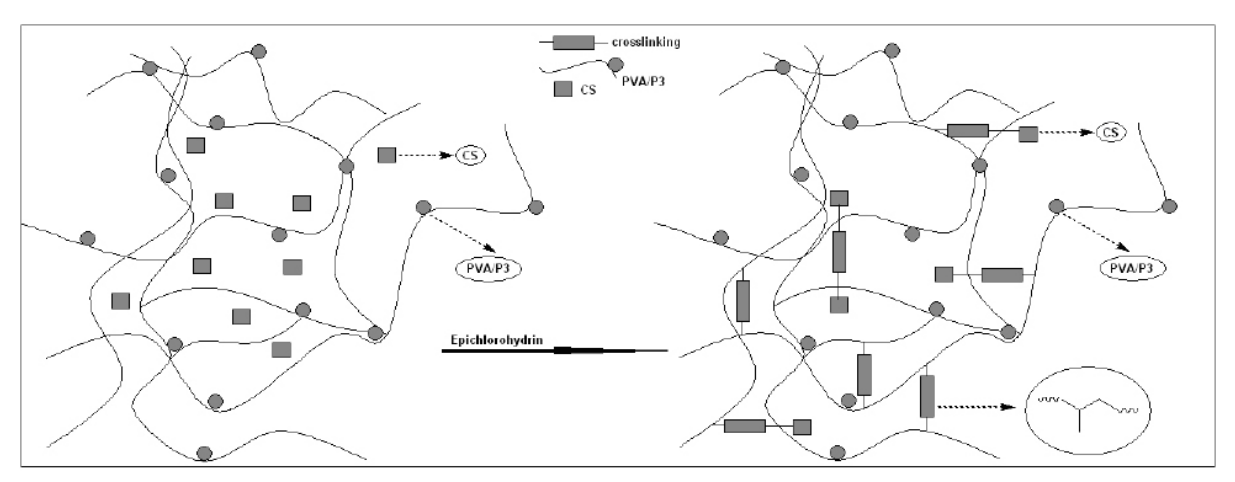


Figure 2. Schematic representation of the formation of the hybrid PVA/PPE (P3)–CS semi-IPN hydrogels.

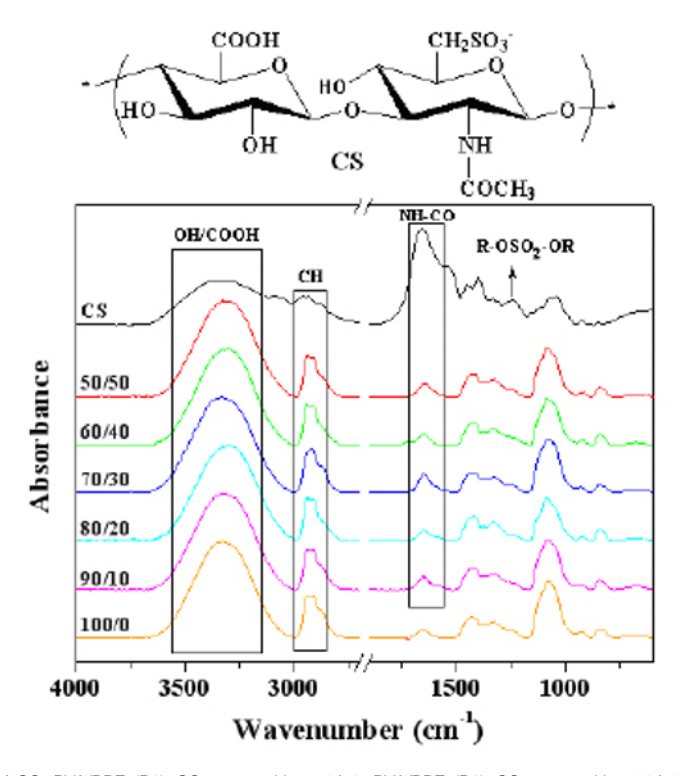


Figure 3. FT-IR spectra of CS, PVA/PPE (P3)–CS composition 50/50, PVA/PPE (P3)–CS composition 60/40, PVA/PPE (P3)–CS composition 70/30, PVA/PPE (P3)–CS composition 80/20, PVA/PPE (P3)–CS composition 90/10, PVA/PPE (P3)–CS composition 100/0.

effect. The structure of hydrogels shown in Fig. 4f is rough and filled with interconnected circular or elliptical macropores. Porous structures were also observed in Figs. 4a-4e but these structures were less rough, and the pores were smaller.

3.3.3. Swelling studies

The swelling behavior, as a main characteristic parameter for hydrogels, depends on the nature of the polymers (nature of charge, ionization capacity of hydrogel in pH, permeability of molecules in

solution, crosslinking density in hydrogel *etc.*) and the environmental conditions (pH and temperature of the medium). Actually, the swelling phenomenon can be universally observed upon appropriate combinations of polymer matrices and solvents. The polymer network comes in contact with the solvent and it starts to swell due to the thermodynamic compatibility of the polymer chains and solvent. Thus, the swelling forces are counterbalanced by the retractive forces induced by the crosslinks of the networks, swelling equilibrium being reached when these forces become equal. On the other

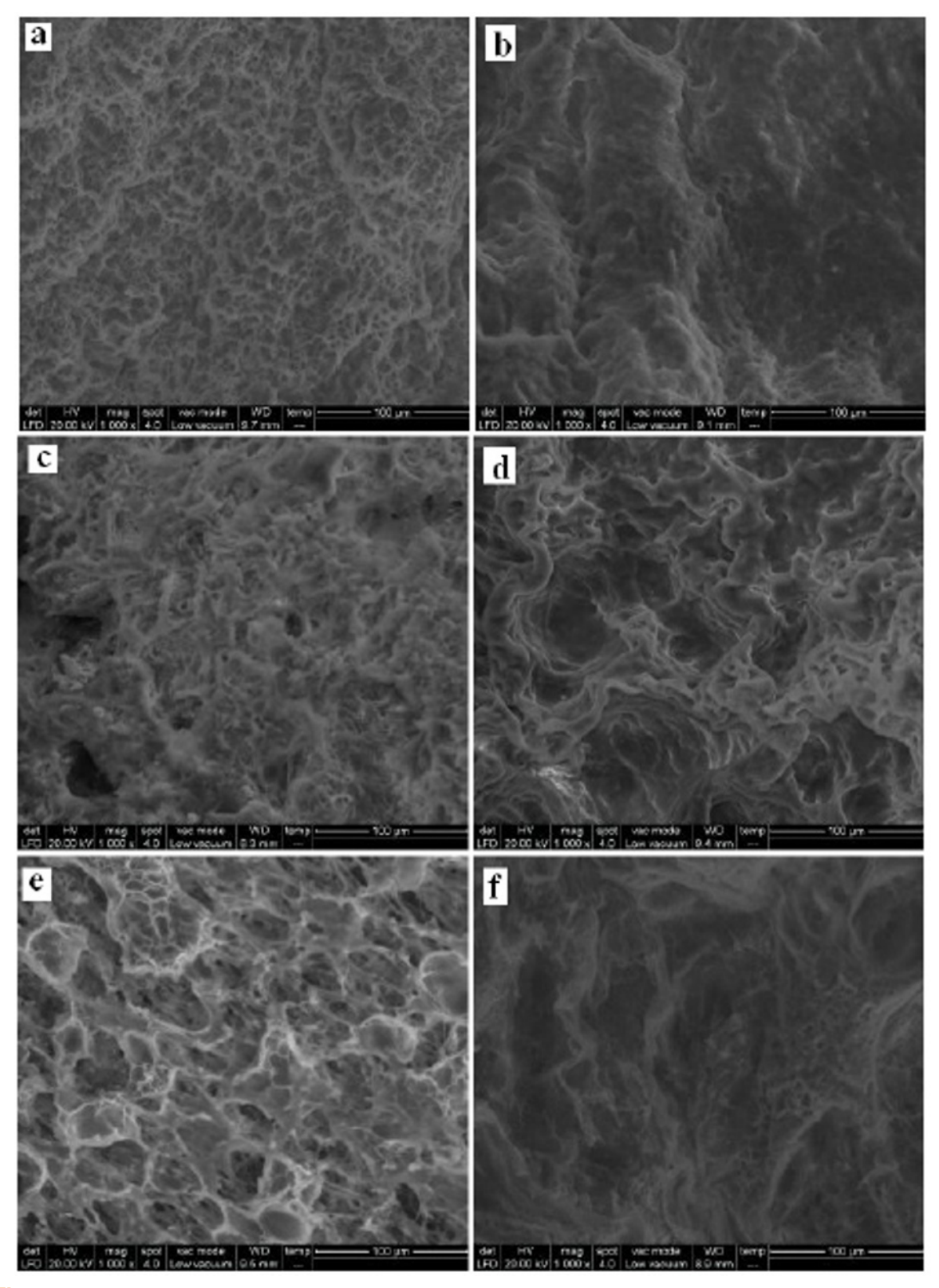


Figure 4. SEM micrographs of the pure PVA/PPE (P3) sample (a), PVA/PPE (P3)—CS composition 90/10 (b), PVA/PPE (P3)—CS composition 80/20 (c), PVA/PPE (P3)—CS composition 70/30 (d), PVA/PPE (P3)—CS composition 60/40 (e), and PVA/PPE (P3)—CS composition 50/50 (f) hydrogels.

Table 1. Yield and pore dimensions for PVA/PPE (P3)–CS hydrogels.

Compositions (%)	Yield (%)	Pores diameters (μm)	
100/0 PVA/PPE (P3)	89	60.28 ± 0.62	
90/10 PVA/PPE (P3)-CS	78	57.3 ± 0.5	
80/20 PVA/PPE (P3)-CS	76	36.6 ± 0.4	
70/30 PVA/PPE (P3)-CS	75	30.7 ± 0.53	
60/40 PVA/PPE (P3)-CS	73	22.34 ± 0.54	
50/50 PVA/PPE (P3)-CS	71	6.15 ± 0.44	

Table 2. Kinetic parameters of swelling for PVA/PPE (P3)–CS semi-IPN hydrogels.

Compositions (%)	n _{sw}	k _{sw} (min ⁻ⁿ)	R
90/10 PVA/PPE (P3)-CS	0.14	0.64	0.99
80/20 PVA/PPE (P3)-CS	0.06	0.92	0.99
70/30 PVA/PPE (P3)-CS	0.01	0.94	0.99
60/40 PVA/PPE (P3)-CS	0.07	0.98	0.99
50/50 PVA/PPE (P3)-CS	0.17	0.98	0.99

hand, the swelling ratio of ionic gels is determined by the electrostatic repulsion between the polymer chains due to the presence of charges on the polymer structure. The extent of the swelling ratio is influenced by pH, ionic strength etc. which reduce the electrostatic repulsion [59].

The chemical composition of PVA/PPE (P3)-CS semi-IPN hydrogels has a significant influence on the swelling ratio. The strong repulsion of negative charges and polar groups cause PVA/PPE (P3)-CS semi-IPN hydrogels to be highly hydrophilic. PVA/PPE (P3)-CS semi-IPN hydrogels are expected to show more capacity of swelling than PVA/PPE network. The absorption of solvent molecules from the environment changes the dimensions of the pores and the physicalchemical properties of the system. Fig. 5 reveals that the swelling occurred rapidly in the first minutes and the swelling ratio of the semi-IPN hydrogels increases with the amount of CS. Only 25 minutes are required to reach the equilibrium swelling ratio for all PPE (P3)-CS semi-IPN hydrogels. Equilibrium swelling capacity for all the samples is high and increases with the content of CS. In PBS at pH 7.4 the high solvent quantity uptake and faster swelling can be attributed to the ionization of -COOH and -CH₂SO₂H groups and anion-anion repulsive electrostatic forces among -COO- and -SO₂groups [60,61].

The initial increase and then the slight decrease for the swelling behavior of the semi-IPN samples can be attributed to screening effect of the counter ions, *i.e.*, NH₄⁺, which shield the charge of -COO⁻ and -SO₃⁻ anions and prevent an efficient repulsion [62].

In Table 2, the kinetic parameters of the swelling process are given for PVA/PPE (P3)–CS semi-IPN hydrogels with various compositions. The values obtained for swelling parameters, $\rm n_{sw}$ varies in range between 0.01-0.17 indicating an anomalous swelling mechanism. The kinetic rate constant, $\rm k_{sw}$ increases with CS content in PVA/PPE (P3) semi-IPN hydrogels from 0.64*min^{-0.14} for 90/10 (PVA/PPE (P3)–CS composition to 0.98*min^{-0.17} for 50/50 (PVA/PPE (P3)–CS composition.

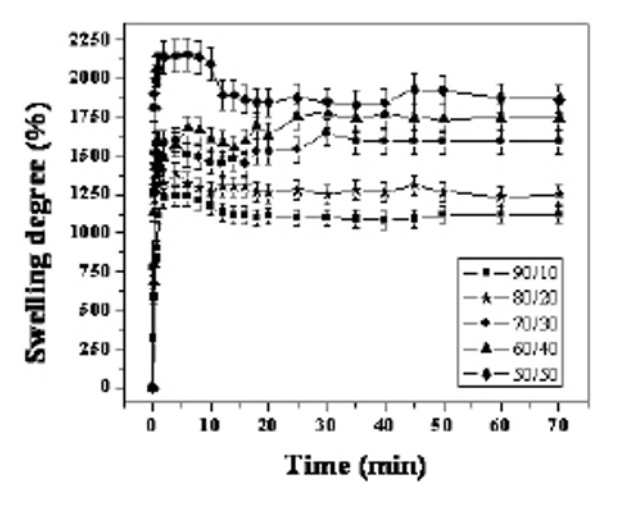
3.3.4. Water vapor sorption capacity

The sorption/desorption isotherms were registered at 25°C from 0 up to 90% relative humidity (RH) by using a IGAsorp equipment. The vapors pressure was increased in 10% humidity steps, with a pre-established equilibrium time of 10 - 20 minutes. For each step, the electromagnetic compensation between tare and sample was used to measure the excedent weight. The desorption isotherms were obtained by gradually decreasing the vapor pressure. The samples were dried prior to measurements at 25°C in flowing nitrogen (250 mL min-1) until a constant value of the weight was reached at RH<1%. Two of them, those for samples 100/0 and 100/30 are illustrative presented in Fig. 6. As can be seen, neither the shape of the isotherm or maximum vapor sorption capacity (Table 3) are significantly affected by the presence of CS in composition.

While the above results of swelling studies reveal a significant rise in water uptake capacity by increasing CS content, a slightly decrease of the sorption capacity (only by 2%) by increasing the CS content could be observed (Table 3). This is due to the different conditions in which the mass transport occurs in the two cases (in liquid water with pH 7.4 and vapour water phase, respectively).

The registered isotherms can be assimilated to those of type III according to Brunauer *et al.* [63], indicating that the results should not be described in terms of free and bound water and of hydration layers. The isotherms show hysteresis between the adsorption and desorption throughout the studied humidity range. In a simplified manner, this could be attributed to a difference in mechanism between condensation and evaporation processes occurring in pores with narrow necks and wide bodies but it is believed that network effects have an important role [64].

Monolayer Brunauer-Emmett-Teller (BET) and multi-layer Guggenheim-Anderson-de Boer (GAB) kinetic models applied to the obtained data on the



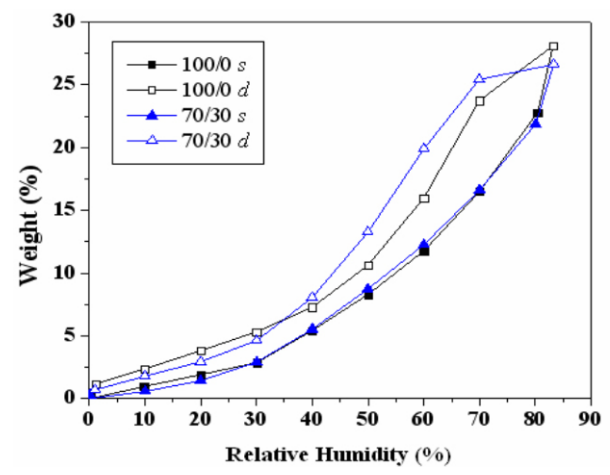


Figure 5. Swelling curves of PVA/PPE (P3)–CS semi-IPN hydrogels in PBS (pH 7.4) at 37°C.

Figure 6. Illustrative shape of the moisture sorption-desorption isotherms.

Table 3. Surface parameters values estimated on the basis of BET and GAB models.

Sample	Weight (%d.b.)	BET model		GAB model	
		A _{BET} (m ² g ⁻¹)	Monolayer (g g ⁻¹)	A _{GAB} (m ² g ⁻¹)	Monolayer (g g ⁻¹)
70/30	26.61	173.78	0.0495	196.77	0.0560
80/20	26.27	139.26	0.0397	158.74	0.0452
90/10	26.38	105.91	0.0302	118.72	0.0338
100/0	28.08	177.24	0.0505	174.83	0.0498

desorption branch gave the values presented in Table 3. It is known that these models have some limitations in the case of water vapor sorption where H-bonding interactions among adsorbed water molecules occur [65,66]. However, the method was also used by other authors [66-68] and the results were compared between them or with those determined by nitrogen sorption. While the BET equation provides an excellent method of estimating surface area only for relative pressures of 0.05 to 0.40 [69], GAB model covers a larger range of humidity, up to 90% and is also used for finding out the monolayer sorption and surface area values. This model describes the water sorption in multilayer well. Values were obtained by applying the two models.

4. Conclusions

Phosphorylated poly(vinyl alcohol) (PVA/PPE) (P1-P4) have been prepared. The formation of the phosphoesteric crosslinks between the chains was confirmed by a spectral study. The value for solid-liquid interfacial tension (5.6 mN m⁻¹) obtained for PVA/PPE (P3) composition, as a result of the presence of the hydrophobic -CH₃ groups

of p-methyl-phenyl phosphonic dichloride is close to the value which describes a good blood-biomaterial compatibility (1-3 mN m⁻¹). The bicomponent hydrogels based on PVA/PPE (P3) polymers and chondroitin sulfate (CS) in various mixing ratios were prepared by chemical crosslinking. The hydrogels display microporous structure, with the pore diameters depending on the CS content. The swelling profiles revealed a dependence on CS content, showing that increasing the CS content in hydrogel compositions leads to a higher swelling ratio. Taking into account the known bio-tolerance of all components involved in the hydrogels structures and their behavior (porosity, wettability, high swelling ratio, and moisture sorption capacity) it is expected that such hydrogels can be applied in the biomedical field.

Acknowledgements

This research was financially suported by European Social Fund – "Cristofor I. Simionescu" Postdoctoral Fellowship Programme (ID POSDRU/89/1.5/S/55216), Sectoral Operational Programme Human Resources Development 2007 – 2013.

References

- [1] A.S. Hoffman, J. Adv. Drug Deliv. Rev. 43, 3 (2002)
- [2] B. Jong, A. Gutowska, Trends. Biotechnol. 20, 3005 (2002)
- [3] A.B. Scranton, B. Rangarajan, J. Klier, J. Adv. Polym. Sci. 122, 1 (1995)
- [4] C.L. Bell, N.A. Peppas, J. Adv. Polym. Sci. 122, 126 (1995)
- [5] M.M. Amiji, Biomaterials 16, 593 (1995)
- [6] W.Y. Chuang, T.H. Young, C.H. Yao, W.Y. Chiu, Biomaterials 20, 1479 (1999)
- [7] T. Koyano, N. Koshizaki, H. Umehara, M. Nagura, N. Minoura, Polymer 41, 4461 (2000)
- [8] J.M. Yang, Y.J. Jong, K.Y. Hsu, J. Biomed. Mater. Res. 35, 175 (1997)
- [9] J.M. Yang, M.C. Wang, Y.G. Hsu, C.H. Chang, S.K. Lo, J. Membr. Sci. 138, 19 (1998)
- [10] J.M. Yang, M.J. Huang, T.S. Yeh, J. Biomed. Mater. Res. 45, 133 (1999)
- [11] P. Gong, L. Zhang, L. Zhuang, J. Lu, J. Appl. Polym. Sci. 68, 1321 (1998)
- [12] C.K. Yeom, K.H. Lee, J. Membr. Sci. 109, 257 (1996)
- [13] D. Myung, D. Waters, M. Wiseman, P. E. Duhamel, J. Noolandi, C. N. Ta, Polym. Adv. Technol 19, 647 (2008)
- [14] C.M. Hassan, N.A. Peppas, Adv. Polym. Sci. 153, 37 (2000)
- [15] C.M. Hassan, J.E. Stewart, N.A. Peppas, Eur. J. Pharm. Biopharm. 49, 161 (2000)
- [16] H.S. Mansur, C.M. Sadahira, A.N. Souza et. Al., Mater. Sci. Eng. C. 28,539 (2008)
- [17] H.L. Lin, Y.F. Liu, T.L. Yu et al, Polymer 46, 5541 (2005)
- [18] N.A. Peppas, S.L. Wright, Eur. J. Pharm. Biopharm 41, 15 (1998)
- [19] A.C. Wenaslau, F.G. Dos Santos, É.R.F. Ramos, C.V. Nakamura, A.F. Rubira, E.C. Muniz, Mat. Sci. Eng. C. Mater. 32, 1259 (2012)
- [20] E.G. Crispim, J.F. Piai, A.R. Fajardo, E.R.F. Ramos, T.U. Nakamura, C.V. Nakamura, A.F. Rubira, E.C. Muniz, eXPRESS Polym. Lett. 6, 383 (2012)
- [21] F.T. Yu, M.D. Yu, W.H. Xian et al., Carbohydr. Polym. 67, 491 (2007)
- [22] K. Juntanon, S. Niamlang, K. Rujirovanit et al., Int. J. Pharm. 356, 1 (2008)
- [23] G. Wu, B. Sue, W. Zhang et al, Mater Chem. Phys 107, 364 (2008)
- [24] J.O. Kim, J.K. Park, J.H. Kim et al, Polymer 45, 7129 (2004)
- [25] A.B. Seabra, M. G. De Oliveira, Biomaterials 25, 3773 (2004)

- [26] A. Moretto, L. Tesolin, F. Marsilio, M. Schiavon, M. Berna, F.M. Veronese, II Farmaco 59, 1 (2004)
- [27] Y.-C. Wang., Y.-Y.Yuan, J.-Z. Du, X.-Z. Yang, J. Wang, Macromol. Biosci. 9, 1154 (2009)
- [28] J. He, P. Ni, S. Wang, H. Shao, M. Zhang, X. Zhu, J. Polym. Sci. Part A: Polym. Chem. 48, 1919 (2010)
- [29] C. Wachiralarpphaithoon, Y. Iwasaki, K. Akiyoshi, Biomaterials 28, 984 (2007)
- [30] J. Liu, W. Huang, Y. Pang, X. Zhu, Y. Zhou, D. Yan, Biomacromolecules 11, 1564 (2010)
- [31] X.-Z. Yang, Y.-C. Wang, L.-Y. Tang, H. Xia, J. Wang, J. Polym. Sci. Part A Polym. Chem. 46, 6425 (2008)
- [32] Z. Zhao, J. Wang, H.Q. Mao, K.W. Leong, Adv. Drug. Deliv. Rev. 55, 483 (2003)
- [33] Y. Iwasaki, K. Akiyoshi, Biomacromolecules 7, 1433 (2006)
- [34] D.A. Wang, C.G. Williams, F. Yang, N. Cher, H. Lee, J.H. Elisseeff, Tissue Eng. 11, 201 (2005)
- [35] N. Inagaki, K. Tomiya, K. Katsuura, Polymer 38, 2057 (1997)
- [36] M. Banks, J.R. Ebdon, M. Johnson, Polymer 34, 4547 (1993)
- [37] N. Hojo, H. Shirai, T. Mori, Kogyo Kagaku Zasshi (J. Chem. Soc., Japan, Ind. Chem.) 74, 273 (1971)
- [38] U. Brasch, W. Burchard, Macromol. Chem. Phys. 197, 223 (1996)
- [39] S. Ito, K. Kawano, M. Mabuchi, M. Yamamoto, Polym. J. 28, 164 (1996)
- [40] D. Darvis, F. Yoshii, K. Makuchi, M. T. Razzak, J. Appl. Polym. Sci. 55, 1619 (1995)
- [41] V. Gimenez, A. Mantecon, V. Cadiz, J. Appl. Polym. Sci. 59, 425 (1996)
- [42] P. Datta, J. Chatterjee, S. Dhara, Colloids Surf. B Biointerf. 94, 177 (2012)
- [43] A.J. Kuijpers, G.H.M. Engbers, T.K.L. Meyvis, S.S.C. de Smedt, J. Demeester, J. Krijgsveld, S.A.J. Zaat, J. Dankert, J. Feijen, Macromolecules 33, 3705 (2000)
- [44] S.-C. Wang, B.-H. Chen, L.-F. Wang, J.-S. Chen, Int. J. Pharm. 329, 103 (2007)
- [45] S. Dawlee, A. Sugandhi, B. Balakrishnan, D. Labarre, A. Jayakrishnan, Biomacromolecules 6, 2040 (2005)
- [46] E.L. Gefter, Fosfororganiceskie monomeri i polimeri, Ed. (Akad Nauk SSSR, Moscow, 1960) (In Russian)
- [47] R. Graff, In: E. Muller, O. Bayer, H. Meerwein, K. Ziegler (Eds.), Methoden der Organischen Chemie (Thieme Georg Verlag, Stuttgart, 1963)
- [48] A.R. Berens, H.B. Hopfenberg, Polymer 19, 489

(1978)

- [49] S. Karpagam, R. Thangaraj, S. Guhanatham, J. Appl. Polym. Sci. 110, 2549 (2008)
- [50] S. Bonakdar, S.H. Emami, M.A. Shokrgozar, A. Farhadi, S.A.H. Ahmadi, A. Amanzadeh Mater. Sci. Eng. C 30, 636 (2010)
- [51] O. Petreus, T. Vlad-Bubulac, G. Cazacu, Mater. Plast. (Bucharest) 42, 115 (2005)
- [52] D. Serbezeanu, T. Vlad-Bubulac, C. Hamciuc, M. Aflori, J. Polym. Sci.: Part A: Polym. Chem. 48, 5391 (2010)
- [53] A.W. Neumann, M.A. Moscarello, W. Zingg, O.S. Hum, S.K. Chang, J. Polym. Sci. Pol. Sym. 66, 391 (1979)
- [54] G. Raffaini, F. Ganazzoli, Macromol. Biosci. 7, 552 (2007)
- [55] J.H. Lee, G. Khang, J.W. Lee, H.B. Lee, J. Colloid Interface Sci. 205, 323 (1998)
- [56] O.M. Paduraru, C. Vasile, S. Patachia, C. Grigoras, A.M. Oprea, Polymery 55, 473 (2010)
- [57] A.-M. Oprea, L. Profire, C.E. Lupusoru, C.M. Chiciuc, D. Ciolacu, C. Vasile, Carbohyd. Polym. 87, 721 (2012)
- [58] H. S. Mansur, R.L. Orefice, A.A.P. Mansur, Polymer 45, 7193 (2004)

- [59] C.-T. Lee, P.-H. Kung, Y.-D. Lee, Carbohydr. Polym. 61, 348 (2005)
- [60] W.D.Comper, O. Zamparo, Biochem. J. 269, 561 (1990)
- [61] X.-N. Shi, W.-B. Wang, A.-Q. Wang, Colloids Surf. B Biointerf. 88, 279 (2011)
- [62] M. Sadeghi, F. Soleimani, H. Shahsavari, N. Ghasemi, J. Basic. Appl. Sci. Res. 2(1), 769 (2012)
- [63] S. Brunauer, L.S. Deming, W.E. Deming, E. Teller, J. Am. Chem. Soc. 62, 1723 (1940)
- [64] IUPAC Recommendations, Pure Appl. Chem. 57, 603 (1985)
- [65] S. Brunauer, P.H. Emmett, E. Teller, J. Am. Chem. Soc. 60, 309 (1938)
- [66] S.L. Wang, C.T. Johnston, D.L. Bish, J.L. White, S.L. Hem, J. Col. Interf. Sci. 260, 26 (2003)
- [67] L. Czepirski, E. Komorowska- Czepirska, J. Szymonska, Appl. Surf. Sci. 196, 150 (2002)
- [68] Z. Sokołowska, J. Jamroz, P. Bańka, Int. Agrophys. 22, 75-80 (2008)
- [69] Y.K. Sung, M.S. Jhon, D.E. Gregonis, J.D. Andrade, Polymer (Korea) 8, 123 (1981)